European Journal of Radiology Open 12 (2024) 100565

Contents lists available at ScienceDirect

European Journal of Radiology Open

journal homepage: www.elsevier.com/locate/ejro

Comparing 2-dimensional versus 3-dimensional MR myelography for cerebrospinal fluid leak detection

Iichiro Osawa [a,*], Takashi Mitsufuji [b], Keita Nagawa [a], Yuki Hara [a], Toshimasa Yamamoto [b], Nobuo Araki [b], Eito Kozawa [a]

[a] Department of Radiology, Saitama Medical University Hospital, 38 Morohongo, Moroyama-machi, Iruma-gun, Saitama 350-0495, Japan
[b] Department of Neurology, Saitama Medical University Hospital, 38 Morohongo, Moroyama-machi, Iruma-gun, Saitama 350-0495, Japan

ARTICLE INFO

Keywords:
Spinal cerebrospinal fluid leak
Spontaneous intracranial hypotension
MRI
MR myelography
3D imaging

ABSTRACT

Purpose: We compared cerebrospinal fluid (CSF) leak conspicuity and image quality as visualized using 3D versus 2D magnetic resonance (MR) myelography in patients with spinal CSF leaks.
Methods: Eighteen patients underwent spinal MR imaging at 3 Tesla. Three board-certified radiologists independently evaluated CSF leak conspicuity and image quality on a 4-point scale; the latter assessed by scoring fat suppression, venous visualization, and severity of CSF flow artifacts. Additionally, the evaluators ranked the overall performances of 2D versus 3D MR myelography upon completing side-by-side comparisons of CSF leak conspicuity. Inter-reader agreement was determined using the Gwet's AC1.
Results: The quality of 3D MR myelography images was significantly better than that of 2D MR myelography with respect to CSF leak conspicuity (mean scores: 3.3 vs. 1.9, $p < 0.0001$) and severity of CSF flow artifacts on the axial view (mean scores: 1.0 vs. 2.5, $p = 0.0001$). Inter-reader agreement was moderate to almost perfect for 2D MR myelography (AC1 = 0.55–1.00), and almost perfect for 3D MR myelography (AC1 = 0.85–1.00). Moreover, 3D MR myelography was judged to be superior to 2D acquisition in 78 %, 83 %, and 83 % of the samples per readers 1, 2 and 3, respectively; the inter-reader agreement was almost perfect (AC1: reader 1 vs. 2; 0.98, reader 2 vs. 3; 0.96, reader 3 vs. 1; 0.98).
Conclusion: CSF leaks are more conspicuous when using 3D MR myelography than when using its 2D counterpart; therefore, the former is more reliable for identifying such leaks.

1. Introduction

Spinal cerebrospinal fluid (CSF) leakage is associated with various conditions including spontaneous intracranial hypotension (SIH) [1], trauma, and medical procedures such as lumbar puncture, epidural injections, and spinal surgery [2]. Detection of CSF leaks is challenging yet essential for prompt treatment. Spinal CSF leaks are evaluated using several techniques such as computed tomography (CT) myelography [3,4], digital subtraction myelography [5], intrathecal gadolinium magnetic resonance (MR) myelography [3,6–8], radioisotope cisternography [9], intravenous enhanced 3D fluid-attenuated inversion recovery (FLAIR) imaging [10,11], and noncontrast MR imaging [4,7,10–13]. The first 4 techniques are invasive given that they require intrathecal injection of contrast material or a radioisotope, and may cause iatrogenic leaks followed by worsening headaches and delayed symptom resolution. FLAIR imaging provides greater sensitivity for detecting subtle T1 shortening induced by gadolinium-based contrast material than T1-weighted imaging [14]. Heavily T2-weighted (T2W) 3D FLAIR is more sensitive to T1 shortening than conventional 3D FLAIR [15], and can detect low concentrations of contrast material incorporated into leaking CSF after intravenous administration [10]. Although this method is less invasive than the former 4 techniques, the use of contrast material is contraindicated for patients with contrast allergy or renal failure.

Abbreviations: CSF, Cerebrospinal fluid; SIH, Spontaneous intracranial hypotension; CT, Computed tomography; MR, Magnetic resonance; FLAIR, Fluid-attenuated inversion recovery; T2W, T2-weighted; TSE, Turbo spin echo; TR, Repetition time; TE, Echo time; SPAIR, Spectral attenuated with inversion recovery; ETL, Echo train length; FOV, Field of view; CHESS, Chemical shift selective; CI, Confidence interval; GRE, Gradient echo.

* Correspondence to: 38 Morohongo, Moroyama-machi, Iruma-gun, Saitama 350-0495, Japan.
E-mail address: oyabun@saitama-med.ac.jp (I. Osawa).

https://doi.org/10.1016/j.ejro.2024.100565
Received 14 February 2024; Received in revised form 11 April 2024; Accepted 15 April 2024

Noncontrast spinal MR imaging is the modality of choice among noninvasive and non-irradiating techniques, and encompasses such methods as turbo spin echo (TSE) T2W imaging [12] and MR myelography [4]. T2W imaging is widely used to pinpoint CSF leaks, which appear as extradural fluid hypersignals; moreover, adding fat suppression techniques to T2W imaging can help differentiate CSF leaks from surrounding fat tissue. MR myelography, which is based on heavily T2W imaging and with which fat suppression is also commonly used, is another approach for detecting CSF leaks and can be performed using either a 2D [4,13,16,17] or 3D [10,11,18–22] acquisition mode. Previous studies have found that 2D MR myelography is comparable to CT myelography [4] or radioisotope cisternography [16] in patients with SIH. However, to our knowledge, no studies have compared 2D versus 3D MR myelography.

The purpose of this study was to compare 3D versus 2D MR myelography for purposes of evaluating spinal CSF leaks. We also assessed the image quality produced by the 2 acquisition methods by evaluating fat suppression, venous visualization, and severity of CSF flow artifacts.

2. Materials and methods

2.1. Patients

This retrospective study was conducted at a single hospital and was approved by the Institutional Review Board. We obtained written informed consent to perform the procedures, while the opt-out method was used in lieu of obtaining informed consent from the patients or their legal guardians to publish the retrospective clinical data. We reviewed the imaging records of 22 consecutive patients who experienced CSF leaks between May 2020 and August 2021 owing to SIH, lumbar puncture, or trauma. The diagnoses of SIH were made according to the criteria proposed by Schievink [23] or the Headache Classification Committee of the International Headache Society (3rd edition) [24]. The latter's criteria were also used to diagnose CSF leaks after lumbar puncture or trauma. Eighteen patients were ultimately included based on the 2 inclusion criteria: 1) fulfilling the diagnostic criteria mentioned above, and 2) undergoing both 2D and 3D MR myelography. None of the patients met the exclusion criterion of insufficient image quality for interpretation.

2.2. MR imaging

All MR examinations were performed in both 2D and 3D at 3 Tesla (MAGNETOM Skyra, Siemens, Erlangen, Germany) with a phased-array spinal coil, and included the cervical-upper thoracic vertebrae (n = 4), lower thoracic-lumbosacral vertebrae (n = 7), and whole (cervical-thoracic-lumbar-sacral) vertebrae (n = 7).

Sagittal, coronal, and 2 oblique (45°) 2D MR myelography scans were performed for all patients with the following parameters: repetition time (TR) 4000 ms, echo time (TE) 1000 ms, spectral attenuated with inversion recovery (SPAIR) fat suppression, flip angle 120°, echo train length (ETL) 314, acquisition matrix size 448 × 314, field of view (FOV) 350 × 350 mm, number of slices 128, 0.8 × 0.8 mm in-plane resolution at 50 mm slice thickness, bandwidth 167 Hz/pixel, an acceleration factor 2 using the GRAPPA parallel imaging technique, number of excitations 1, and acquisition time 9 s in each plane (total, 36 s).

Axial 2D MR myelography was performed for 16 patients using the following parameters: TR 5000 ms, TE 1000 ms, SPAIR fat suppression, flip angle 120°, ETL 314, acquisition matrix size 448 × 314, FOV 200 × 200 mm, number of slices 35, 0.4 × 0.4 mm in-plane resolution at 6 mm slice thickness, bandwidth 167 Hz/pixel, an acceleration factor 2 using the GRAPPA parallel imaging technique, number of excitations 1, and acquisition time 3 min 2 s.

3D MR myelography in the sagittal plane was performed with the following parameters based on a previous study [10]: TR 4400 ms, TE 425 ms, frequency-selective (chemical shift selective [CHESS]) fat suppression, average flip angle 110°, ETL 519, acquisition matrix size 384 × 384, FOV 350 × 350 mm, number of slices 128, 0.9 × 0.9 mm in-plane resolution at 0.9 mm slice thickness, bandwidth 434 Hz/pixel, an acceleration factor 2 using the GRAPPA parallel imaging technique, number of excitations 1.4, and acquisition time 3 min 42 s. We generated axial and coronal multiplanar reconstruction images with a slice thickness of 0.9 mm.

We compared sagittal, coronal, and 2 oblique 2D myelography to sagittal and coronal reformatted 3D myelography. We also compared axial 2D myelography to axial reformatted 3D myelography.

2.3. Imaging analysis

The images were analyzed by subjectively evaluating CSF leak conspicuity and image quality. All images were reviewed independently by three board-certified radiologists (I.O., K.N., and Y.H.), who were blinded to the clinical information and sequence parameters, in random order.

CSF leak conspicuity was assessed for epidural and paraspinal fluid collection. Epidural fluid collection was reflected by fluid signal intensity within the epidural space; in particular, subtle arched hyperintensity in the interspinous epidural space was termed the "Dinosaur tail sign" based on its shape [4,13,16,17]. Paraspinal fluid collection was defined as a fluid signal in any space adjacent to but outside the spine, including abnormal intensity around the nerve root sleeve and within the retrospinal space at C1–2. Retrospinal fluid collection at C1–2 was referred to as the C1–2 sign [25].

CSF leak conspicuity was graded on a 4-point scale as follows: 1 = CSF leak was inconspicuous or minimally visible with poor contrast between the leak and surrounding structures, 2 = CSF leak was visible with moderate contrast between the leak and surrounding structures, 3 = CSF leak was visible with good contrast between the leak and surrounding structures, and 4 = CSF leak was sharply visible with excellent contrast between the leak and surrounding structures. When multiple leaks were present in the epidural and paraspinal spaces at the C/T/L/S levels, the readers provided a single overall score for all leaks combined.

Fat suppression, venous visualization, and severity of CSF flow artifacts were graded using a 4-point-scale to assess image quality. Grading for fat suppression was as follows: 1 = poor with severe effect on image interpretation, 2 = moderate with some non-severe effect on image interpretation, 3 = good with no effect on image interpretation, and 4 = excellent with no effect on image interpretation. Evaluation of fat suppression focused on epidural and paraspinal fat. Grading for venous visualization was as follows: 1 = invisible or minimally visible with no effect on image interpretation, 2 = visible with no effect on image interpretation, 3 = visible with some non-severe effect on image interpretation, and 4 = clearly visible with severe effect on image interpretation. Evaluation of venous suppression focused on veins in the paraspinal area, including the anterior and posterior external vertebral venous plexus, intervertebral vein, and interspinous vein. Grading for severity of CSF flow artifacts was as follows: 1 = no artifacts, 2 = minor artifacts with no effect on diagnostic image quality, 3 = moderate artifacts with some non-severe diagnostic image quality, and 4 = unacceptable artifacts with severe diagnostic image quality.

We assessed images in axial and non-axial directions separately owing to potential differences between the CSF flow artifacts in the originally acquired axial plane and those in the non-axial planes on 2D MR myelography. At the end of the session, both series for each patient were presented to the 3 readers side-by-side, and each reader selected their preferred sequence for CSF leak conspicuity.

2.4. Statistical analysis

For subjective analyses, the scores of 3 readers were averaged, and the Wilcoxon signed-rank test was used to assess statistical differences

between 2D and 3D MR myelography. Inter-reader agreement of the subjective analyses was assessed using the Gwet's AC1, which was selected instead of Cohen's kappa because the former overcomes the limitation of the kappa value being sensitive to trait prevalence and marginal probability [26]. AC1 values < 0 indicated no agreement whereas scores of 0–0.20, 0.21–0.40, 0.41–0.60, 0.61–0.80, and 0.81–1 indicated slight, fair, moderate, substantial, and almost perfect agreement, respectively [27]. Two-tailed *p*-values < 0.05 were considered statistically significant. All statistical calculations were performed using the statistical computing language R (version 4.0.5; http//www.r-project.org/).

3. Results

3.1. Patients

The patients' characteristics are shown in Table 1. The cohort included 6 male and 12 female patients; their average age was 33 years (range, 13–61 years). The etiologies of CSF leaks included SIH (n = 14), lumbar puncture (n = 3), and trauma (n = 1).

3.2. Comparison of CSF leak conspicuity and image quality

Table 2 summarizes the subjective comparison of CSF leak conspicuity and image quality using 4-point scales. The 3 reader's scores for CSF leak conspicuity were significantly higher for 3D than for 2D MR myelography ($p < 0.0001$) (Figs. 1-3). Fat suppression scores were significantly higher on 2D than on 3D MR myelography ($p < 0.0001$). Venous visualization scores were significantly higher on 3D than on 2D MR myelography ($p < 0.0001$). Moreover, 3D MR myelography showed fewer CSF flow artifacts than axial 2D MR myelography ($p = 0.0001$) (Fig. 2). Inter-reader agreement was moderate to almost perfect for 2D MR myelography (AC1 = 0.55–1.00), and almost perfect for 3D MR myelography (AC1 = 0.85–1.00).

3.3. Side-by-side comparison of CSF leak conspicuity

As shown in Table 3, subjective comparisons of CSF leak conspicuity performed side-by-side revealed that 3D MR myelography was equal or superior to 2D MR myelography in 100 % of the cases for the 3 readers. Inter-reader agreement was almost perfect (Reader 1 vs. 2: AC1 = 0.98, 95 % CI [confidence interval] = 0.94–1.02; Reader 2 vs. 3: AC1 = 0.96, 95 % CI = 0.90–1.02; Reader 3 vs. 1: AC1 = 0.98, 95 % CI = 0.94–1.02).

4. Discussion

Our study found 3D MR myelography to be superior to 2D MR myelography in terms of CSF leak conspicuity. Moreover, 3D MR myelography exhibited fewer CSF flow artifacts but was inferior to the 2D sequence in terms of the quality of fat suppression. MR myelography is based on a heavily T2W imaging technique, and includes the TSE [4,10,13,16,17,20,21] and gradient echo (GRE) sequences [18,19,22]; TSE sequences are performed using 2D or 3D acquisition. The 2D TSE sequence consists of single-slice MR myelography [4,13,16,17]

Table 1
Clinical and spinal magnetic resonance imaging characteristics of patients with cerebrospinal fluid leakage (n = 18).

Patient No.	Age (years)	Sex	Etiology	Symptoms	Examined range of 2D MR myelography		Spinal MR imaging findings	
					Coronal, sagittal, and 2 oblique	Axial	Epidural fluid collection (location)	Paraspinal fluid collection (location)
1	60	F	SIH	Orthostatic headache	Lower T/L/S	NA	+ (S)	-
2	59	F	Iatrogenic (epidural anesthesia)	Orthostatic headache, nausea	W	NA	+ (T/L)	-
3	14	F	SIH	Headache	Lower T/L/S	Lower T/L/S	+ (S)	-
4	61	F	SIH	Feeling of pressure within the head	W	W	+ (T)	-
5	31	M	SIH	Headache	W	W	+ (C/T/L/S)	+ (C/T/L/S)
6	18	F	Iatrogenic (lumbar puncture)	Headache	Lower T/L/S	Lower T/L/S	+ (L)	-
7	16	M	SIH	Headache	Lower T/L/S	Lower T/L/S	+ (S)	-
8	17	M	SIH	Orthostatic headache	Lower T/L/S	Lower T/L/S	+ (S)	-
9	32	F	SIH	Headache, vertigo	C/upper T	C/upper T	+ (C/upper T)	-
10	25	F	SIH	Headache, vertigo	Lower T/L/S	Lower T/L/S	+ (S)	-
11	38	F	SIH	Headache	Lower T/L/S	Lower T/L/S	+ (S)	-
12	42	F	SIH	Orthostatic headache	C/upper T	C/upper T	+ (C/upper T)	-
13	13	M	Trauma	Orthostatic headache	W	W	+ (S)	-
14	13	F	SIH	Orthostatic headache	W	W	+ (S)	-
15	49	F	SIH	Orthostatic headache	C/upper T	C/upper T	+ (C/upper T)	-
16	19	M	Iatrogenic (lumbar puncture)	Headache	W	W	+ (L/S)	-
17	40	M	SIH	Orthostatic headache	W	W	+ (C/T/L/S)	+ (C)
18	45	F	SIH	Orthostatic headache	C/upper T	C/upper T	+ (C/upper T)	-

SIH spontaneous intracranial hypotension, *NA* not available, *C* cervical spine, *T* thoracic spine, *L* lumbar spine, *S* sacral spine, *W* whole spine

Table 2
Comparison of cerebrospinal fluid leak conspicuity and image quality between 2D and 3D magnetic resonance myelography.

		n	Comparison using 4-point scale			AC1 (95 % CI)					
			Mean ± SD		*p*-value	Reader 1 vs. 2		Reader 2 vs. 3		Reader 3 vs. 1	
			2D	3D		2D	3D	2D	3D	2D	3D
CSF leak conspicuity		18	1.9 ± 0.8	3.3 ± 0.5	< 0.0001	0.95 (0.89–1.00)	0.94 (0.88–0.99)	0.93 (0.86–1.00)	0.85 (0.72–0.98)	0.88 (0.79–0.97)	0.90 (0.84–0.96)
Fat suppression		18	3.8 ± 0.3	2.5 ± 0.6	< 0.0001	0.98 (0.95–1.01)	0.96 (0.91–1.01)	0.95 (0.91–1.00)	0.93 (0.88–0.99)	0.97 (0.94–1.01)	0.90 (0.78–1.02)
Venous visualization		18	1.0 ± 0.1	2.6 ± 0.5	< 0.0001	0.99 (0.98–1.01)	0.92 (0.87–0.98)	1.00 (1.00–1.00)	0.95 (0.89–1.00)	0.99 (0.98–1.01)	0.95 (0.90–1.00)
Severity of CSF flow artifacts	Sagittal, coronal, and 2 oblique 2D vs. sagittal and coronal reformatted 3D	18	1.0 ± 0.0	1.0 ± 0.0	NA	1.00 (1.00–1.00)	1.00 (1.00–1.00)	1.00 (1.00–1.00)	1.00 (1.00–1.00)	1.00 (1.00–1.00)	1.00 (1.00–1.00)
	Axial 2D vs. axial reformatted 3D	16	2.5 ± 0.9	1.0 ± 0.0	0.0001	0.55 (0.25–0.84)	1.00 (1.00–1.00)	0.75 (0.56–0.93)	1.00 (1.00–1.00)	0.86 (0.75–0.97)	1.00 (1.00–1.00)

CSF cerebrospinal fluid, *SD* standard deviation, *CI* confidence interval, *NA* not available

Fig. 1. A 31-year-old man with spontaneous intracranial hypotension (patient 5). Sagittal 2D magnetic resonance (MR) myelography (**a**) partially depicts epidural fluid collection located in the interspinous area at L2–3 (arrowhead). Sagittal 3D MR myelography (**b**) demonstrates epidural fluid collection distributed more widely from T12–L1 to L3–4 (arrowheads); this is termed the "Dinosaur tail sign". On axial 2D MR myelography (**c**), epidural fluid collection is inconspicuous at T4. On axial reformatted 3D MR myelography (**d**), epidural fluid collection (arrow) is visible with the dura mater (small arrows) ventrally appearing as a thin hypointense layer.

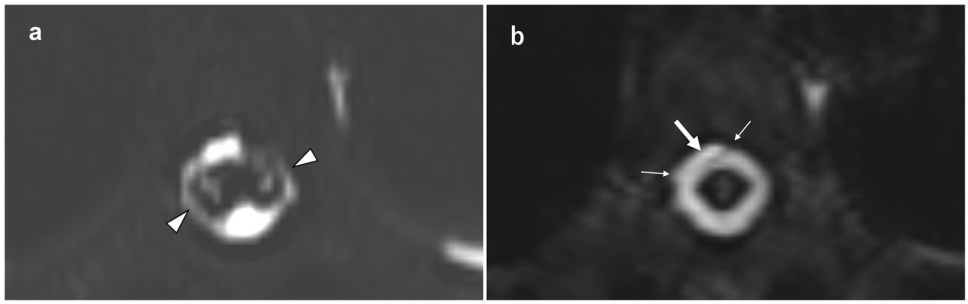

Fig. 2. A 61-year-old woman with spontaneous intracranial hypotension (patient 4). Axial 2D magnetic resonance (MR) myelography (**a**) shows prominent cerebrospinal fluid (CSF) artifacts (arrowheads), which obscure the dura mater at T7. Axial reformatted 3D MR myelography (**b**) reduces the CSF flow artifacts and clearly depicts epidural fluid collection (arrow) as well as the dura mater (small arrows).

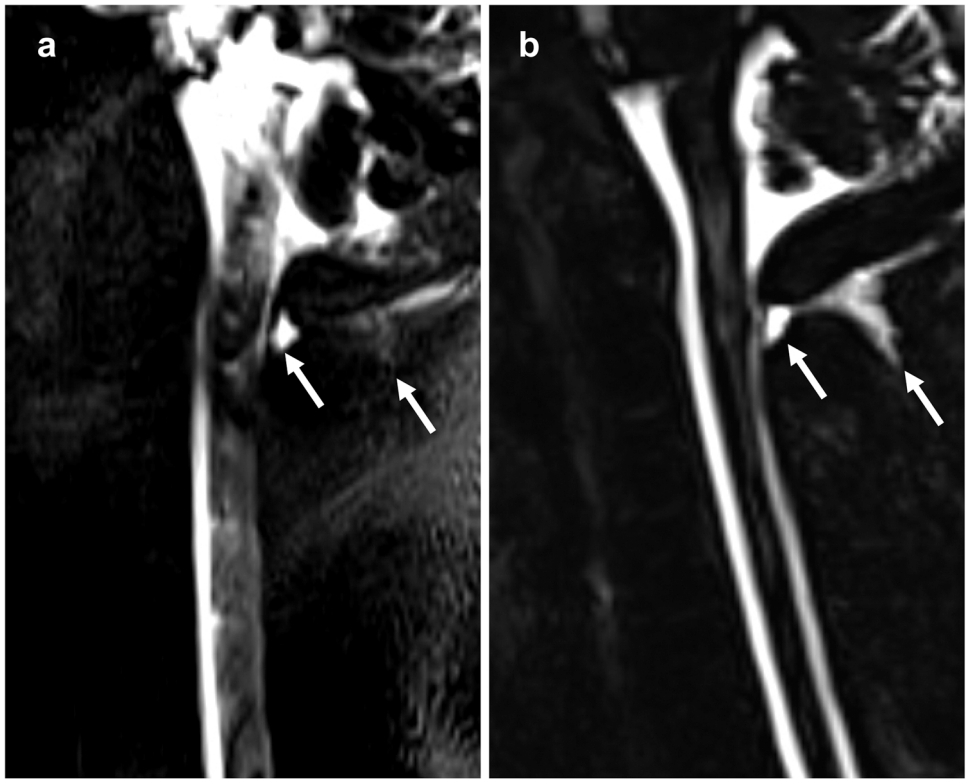

Fig. 3. A 31-year-old man with spontaneous intracranial hypotension (patient 5, the same patient shown in Fig. 1). Sagittal 2D magnetic resonance (MR) myelography (**a**) shows retrospinal fluid collection (arrows) at C1–2 (C1–2 sign). Sagittal 3D MR myelography (**b**) depicts C1–2 sign (arrows) more conspicuously, likely because of the higher spatial resolution.

Table 3
Side-by-side comparison of cerebrospinal fluid leak conspicuity when using 2D versus 3D magnetic resonance myelography (n = 18).

		Reader 1			Reader 2			Reader 3		
	n	2D	Equal	3D	2D	Equal	3D	2D	Equal	3D
CSF leak conspicuity	18	0	4	14	0	3	15	0	3	15
Percentage		0	22	78	0	17	83	0	17	83

CSF cerebrospinal fluid

characterized by a single-shot TSE sequence and extremely long effective TE. Long effective TE provides excellent suppression of background signals from fat or veins. A single-shot sequence in a coronal or sagittal direction allows for the delineation of the entire spine in a single projection image within a shorter scanning time, and does not require a postprocessing procedure such as maximum intensity projection. However, a single projection image cannot be reconstructed in other directions, which makes additional image acquisitions necessary at the desired angles. Furthermore, 2D single thick-slice MR myelography may not have the capacity to differentiate between epidural CSF leaks and subarachnoid CSF, particularly on coronal images, because low spatial resolution obscures details in the dura mater between the 2 fluid-filled spaces.

In contrast, 3D sequences include TSE [10,20,21] and steady-state

GRE [18,19]. While 3D sequences require a relatively longer acquisition time than 2D sequences, a 3D isotropic dataset can generate multiplanar reconstruction images of arbitrarily reformatted directions. The 3D TSE sequence with a variable flip angle refocusing pulse is a variant that reduces the blur and specific absorption rate under a very long applied ETL. This sequence is now available from several MR equipment manufacturers such as SPACE (Siemens) [10], BRAINVIEW (Philips) [28], and CUBE (General Electric). In contrast, the 3D steady-state GRE sequence uses steady states of magnetizations and produces submillimeter spatial resolution with a high CSF-to-soft tissue contrast in short scanning times.

There are few reports about the comparative analysis of CSF leak detection between noncontrast heavily T2W imaging and other MR imaging. Osawa et al. assessed the clinical utility of intravenous enhanced heavily T2W 3D FLAIR imaging by comparing the visualization of CSF leaks to 3D MR myelography in patients with SIH [10]. The authors concluded that contrast-enhanced heavily T2W 3D FLAIR imaging was superior to 3D MR myelography. Dobrocky et al. compared the diagnostic accuracy of 2 different noncontrast MR imaging (T2W imaging and fat-saturated 3D heavily T2W imaging) and intrathecal enhanced MR myelography for CSF leak detection in patients with SIH [29]. These authors concluded that intrathecal enhanced MR myelography was nonsuperior to noncontrast MR imaging and provided no significant diagnostic benefit in the standard evaluation of spinal CSF leaks.

We selected the T2W 3D SPACE sequence for 3D MR myelography along with CHESS fat suppression, where axial reformatting of the sagittal dataset reduces the CSF flow artifacts that are more problematic in the originally acquired axial sections than in the sagittal sections [30]. Epidural fluid collection was more conspicuous on 3D than on 2D MR myelography in the present study likely because of the higher spatial resolution and reduced CSF flow artifacts. Three factors that are critical for identifying epidural fluid collection [10] include 1) detection of the dura mater, 2) a sufficient volume of leaked CSF, and 3) differentiation of epidural fat from CSF. The higher spatial resolution provided by 3D MR myelography can improve the detection of the dura matter and even identify a small volume of leaked CSF. Flow artifacts within the CSF in the subarachnoid space can obscure the dura mater, which is a thin structure located between the subarachnoid space and epidural space. As such, 3D MR myelography has the potential to reduce CSF flow artifacts and detect the dura matter more readily.

Paraspinal fluid collection also was more conspicuous on 3D than on 2D MR myelography in the current study, a possible explanation for which is the higher spatial resolution provided by 3D MR myelography. When identifying paraspinal fluid collection, it is critical to differentiate leaked CSF from paraspinal fat, veins, and other fluid-filled structures (e.g., cystic dilatation of nerve root sleeve, meningeal diverticula, and facet joint effusion). Although the 2D sequence was superior to its 3D counterpart in terms of fat suppression quality and showed lower venous visualization scores, it nevertheless offered less anatomical information than the latter owing to the suppression of the background signal, which may make it difficult to differentiate CSF leaks from these fluid-filled structures.

There were certain limitations to our study. First, it was retrospective in nature and included a small sample size. Second, MR parameters were optimized to allow acceptable acquisition time in clinical practice, and were therefore not similar between the sequences. The fat suppression techniques also differed between the sequences, as 2D and 3D MR myelography employed CHESS and SPAIR, respectively. Since SPAIR is less susceptible to B1 heterogeneity than CHESS because of its adiabatic pulse [31], this technique can typically provide more homogenous fat suppression. Thus, the superiority of 2D MR myelography for fat suppression may be owing to the use of SPAIR in addition to the very long TE. Finally, it was unclear whether the detected CSF leaks represented the exact sites of the dural defects. Further studies should compare these modalities to standard procedures such as CT myelography.

5. Conclusion

We found 3D MR myelography to be superior to 2D acquisition in terms of CSF leak conspicuity, and therefore deem it more suitable for identifying spinal CSF leaks.

Funding

This research was supported by JSPS KAKENHI under Grant Number JP22K15807, Health and Labour Sciences Research Grants under Grant Number 23GC1002, and Grand-in-Aid from Saitama Medical University Internal Research under Grant Number 21-B-1–05.

Ethical statement

All procedures performed in studies involving human participants were in accordance with the ethical standards of the institutional and/or national research committee and with the 1964 Helsinki declaration and its later amendments or comparable ethical standards.

Informed consent

This retrospective study was conducted at a single institution and approved by the Institutional Review Board of our institution. We obtained written informed consent for the procedures and opt-out consent for the use of retrospective clinical data from all patients/ from parents or legal guardian of patient less than 18 years.

CRediT authorship contribution statement

Nobuo Araki: Writing – review & editing, Supervision. **Toshimasa Yamamoto:** Writing – review & editing, Supervision. **Yuki Hara:** Writing – review & editing, Formal analysis. **Keita Nagawa:** Writing – review & editing, Formal analysis. **Eito Kozawa:** Writing – review & editing, Supervision. **Takashi Mitsufuji:** Writing – review & editing, Supervision, Data curation. **Iichiro Osawa:** Writing – original draft, Methodology, Formal analysis, Data curation, Conceptualization.

Declaration of Competing Interest

The authors declare that they have no conflict of interest.

Acknowledgments

None.

References

[1] W.I. Schievink, Spontaneous spinal cerebrospinal fluid leaks and intracranial hypotension, Jama 295 (19) (2006) 2286–2296.
[2] Y.F. Wang, J.L. Fuh, J.F. Lirng, S.P. Chen, S.S. Hseu, J.C. Wu, S.J. Wang, Cerebrospinal fluid leakage and headache after lumbar puncture: a prospective non-invasive imaging study, Brain 138 (Pt 6) (2015) 1492–1498.
[3] J.L. Chazen, J.F. Talbott, J.E. Lantos, W.P. Dillon, MR myelography for identification of spinal CSF leak in spontaneous intracranial hypotension, AJNR Am. J. Neuroradiol. 35 (10) (2014) 2007–2012.
[4] Y.F. Wang, J.F. Lirng, J.L. Fuh, S.S. Hseu, S.J. Wang, Heavily T2-weighted MR myelography vs CT myelography in spontaneous intracranial hypotension, Neurology 73 (22) (2009) 1892–1898.
[5] J.M. Hoxworth, T.L. Trentman, A.L. Kotsenas, K.R. Thielen, K.D. Nelson, D. W. Dodick, The role of digital subtraction myelography in the diagnosis and localization of spontaneous spinal CSF leaks, AJR, Am. J. Roentgenol. 199 (3) (2012) 649–653.
[6] S. Albayram, F. Kilic, H. Ozer, S. Baghaki, N. Kocer, C. Islak, Gadolinium-enhanced MR cisternography to evaluate dural leaks in intracranial hypotension syndrome, AJNR Am. J. Neuroradiol. 29 (1) (2008) 116–121.
[7] J.H. Medina, K. Abrams, S. Falcone, R.G. Bhatia, Spinal imaging findings in spontaneous intracranial hypotension, AJR, Am. J. Roentgenol. 195 (2) (2010) 459–464.

[8] E. Hattingen, R. DuMesnil, U. Pilatus, A. Raabe, T. Kahles, J. Beck, Contrast-enhanced MR myelography in spontaneous intracranial hypotension: description of an artefact imitating CSF leakage, Eur. Radio. 19 (7) (2009) 1799–1808.
[9] B. Mokri, Radioisotope cisternography in spontaneous CSF leaks: interpretations and misinterpretations, Headache 54 (8) (2014) 1358–1368.
[10] I. Osawa, E. Kozawa, T. Mitsufuji, T. Yamamoto, N. Araki, K. Inoue, M. Niitsu, Intravenous enhanced 3D FLAIR imaging to identify CSF leaks in spontaneous intracranial hypotension: comparison with MR myelography, Eur. J. Radio. Open 8 (2021) 100352.
[11] I. Osawa, Diagnostic imaging of cerebrospinal fluid hypovolemia: the evolution of magnetic resonance imaging and image interpretation (in Japanese), Auton. Nerveous Syst. 60 (4) (2023) 161–171.
[12] A. Watanabe, T. Horikoshi, M. Uchida, H. Koizumi, T. Yagishita, H. Kinouchi, Diagnostic value of spinal MR imaging in spontaneous intracranial hypotension syndrome, AJNR Am. J. Neuroradiol. 30 (1) (2009) 147–151.
[13] P.H. Tsai, J.L. Fuh, J.F. Lirng, S.J. Wang, Heavily T2-weighted MR myelography in patients with spontaneous intracranial hypotension: a case-control study, Cephalalgia 27 (8) (2007) 929–934.
[14] I. Osawa, E. Kozawa, Y. Yamamoto, S. Tanaka, T. Shiratori, A. Kaizu, K. Inoue, M. Niitsu, Contrast enhancement of the normal infundibular recess using heavily T2-weighted 3D Flair, Magn. Reson. Med. Sci. 21 (3) (2022) 469–476.
[15] I. Osawa, E. Kozawa, S. Tanaka, A. Kaizu, K. Inoue, T. Ikezono, T. Fujimaki, M. Niitsu, Signal and morphological changes in the endolymph of patients with vestibular schwannoma on non-contrast 3D FLAIR at 3 Tesla, BMC Med. Imaging 21 (1) (2021) 135.
[16] H.M. Yoo, S.J. Kim, C.G. Choi, D.H. Lee, J.H. Lee, D.C. Suh, J.W. Choi, K.S. Jeong, S.J. Chung, J.S. Kim, S.C. Yun, Detection of CSF leak in spinal CSF leak syndrome using MR myelography: correlation with radioisotope cisternography, AJNR Am. J. Neuroradiol. 29 (4) (2008) 649–654.
[17] K. Sakurai, M. Kanoto, M. Nakagawa, M. Shimohira, A.M. Tokumaru, M. Kameyama, K. Shimoji, S. Morimoto, N. Matsukawa, M. Nishio, Y. Shibamoto, Dinosaur tail sign: a useful spinal MRI finding indicative of cerebrospinal fluid leakage, Headache 57 (6) (2017) 917–925.
[18] I. Yousry, S. Förderreuther, B. Moriggl, M. Holtmannspötter, T.P. Naidich, A. Straube, T.A. Yousry, Cervical MR imaging in postural headache: MR signs and pathophysiological implications, AJNR Am. J. Neuroradiol. 22 (7) (2001) 1239–1250.
[19] H.J. Koo, S.J. Kim, S.J. Chung, S.-C. Rhim, Detection of surgery-related spinal cerebrospinal fluid leakage using magnetic resonance myelography, J. Korean Soc. Magn. Reson. Med. 17 (2) (2013) 149–153.
[20] Y. Tomoda, Y. Korogi, T. Aoki, T. Morioka, H. Takahashi, M. Ohno, I. Takeshita, Detection of cerebrospinal fluid leakage: initial experience with three-dimensional fast spin-echo magnetic resonance myelography, Acta Radio. 49 (2) (2008) 197–203.
[21] C.H. Chen, J.H. Chen, H.C. Chen, J.W. Chai, P.L. Chen, C.C. Chen, Patterns of cerebrospinal fluid (CSF) distribution in patients with spontaneous intracranial hypotension: assessed with magnetic resonance myelography, J. Chin. Med. Assoc. 80 (2) (2017) 109–116.
[22] H.J. Koo, S.J. Kim, S.J. Chung, S.-C. Rhim, Detection of surgery-related spinal cerebrospinal fluid leakage using magnetic resonance myelography, J. Korean Soc. Magn. Reson. Med. 17 (2) (2013) 149–153.
[23] W.I. Schievink, D.W. Dodick, B. Mokri, S. Silberstein, M.G. Bousser, P.J. Goadsby, Diagnostic criteria for headache due to spontaneous intracranial hypotension: a perspective, Headache 51 (9) (2011) 1442–1444.
[24] International Classification of Headache Disorders, Headache classification committee of the international headache society (IHS) The international classification of headache disorders, Cephalalgia 38 (1) (2018) 1–211.
[25] W.I. Schievink, M.M. Maya, J. Tourje, False localizing sign of C1-2 cerebrospinal fluid leak in spontaneous intracranial hypotension, J. Neurosurg. 100 (4) (2004) 639–644.
[26] K.L. Gwet, Computing inter-rater reliability and its variance in the presence of high agreement, Br. J. Math. Stat. Psychol. 61 (Pt 1) (2008) 29–48.
[27] J.R. Landis, G.G. Koch, The measurement of observer agreement for categorical data, Biometrics 33 (1) (1977) 159–174.
[28] I. Osawa, K. Nagawa, Y. Hara, H. Shimizu, S. Tanaka, E. Kozawa, Utility of contrast-enhanced 3D STIR FLAIR imaging for evaluating pituitary adenomas at 3 Tesla, Eur. J. Radio. Open 11 (2023) 100500.
[29] T. Dobrocky, A. Winklehner, P.S. Breiding, L. Grunder, G. Peschi, L. Häni, P. J. Mosimann, M. Branca, J. Kaesmacher, P. Mordasini, A. Raabe, C.T. Ulrich, J. Beck, J. Gralla, E.I. Piechowiak, Spine MRI in spontaneous intracranial hypotension for CSF leak detection: nonsuperiority of intrathecal Gadolinium to heavily T2-weighted fat-saturated sequences, AJNR Am. J. Neuroradiol. 41 (7) (2020) 1309–1315.
[30] F.H. Chokshi, G. Sadigh, W. Carpenter, J.W. Allen, Diagnostic quality of 3D T2-space compared with T2-FSE in the evaluation of cervical spine MRI anatomy, AJNR Am. J. Neuroradiol. 38 (4) (2017) 846–850.
[31] F. Del Grande, F. Santini, D.A. Herzka, M.R. Aro, C.W. Dean, G.E. Gold, J. A. Carrino, Fat-suppression techniques for 3-T MR imaging of the musculoskeletal system, Radiographics 34 (1) (2014) 217–233.